



# Spatial appraisal of aquifer characterization through hydrogeophysical investigations in central part of Bari Doab, Punjab, Pakistan

Shahbaz Muhammad · Pervez Khalid · Muhammad Irfan Ehsan

Received: 1 March 2022 / Accepted: 7 October 2022 / Published online: 19 October 2022  
© The Author(s), under exclusive licence to Springer Nature Switzerland AG 2022

**Abstract** The study area lies in Southwestern part of Sahiwal District, Punjab, Pakistan, which is the central part of interfluvial system, i.e., Bari Doab. Hydrogeophysical investigations were carried out for the spatial appraisal of groundwater aquifers resources in the study area through electrical resistivity survey. A total of forty vertical electrical soundings through Schlumberger electrode configuration are conducted in the study area. The interpreted results of electrical resistivity survey along with interactive modeling suggest that four to six numbers of geo-electric layers exist in the subsurface in the study area. The alternating alluvium comprised of silt, sand, gravel, and kanker layers has been interpreted. The interpreted resistivities are categorized from very high to very low in the study area. Below the water table, very low resistivity values interpreted mainly as sand and sand-gravel saturated with saline water. Moreover, the interpretation of our developed maps also leads to demarcate the fresh and saline groundwater zones. Interpreted results decipher that this gigantic saline water zone starts below the depth of 150 m and extends below the depth of 300 m. The models of true resistivities are

also calibrated with the lithological logs of test holes and tube wells within the study area. The sandy and gravel layers are the most promising zones for good-quality groundwater that leads to the development tube wells up to the depth of 150 m within the study area.

**Keywords** Alluvium aquifer · Bari Doab · Hydrostratigraphy · Vertical electrical sounding (VES)

## Introduction

Electrical resistivity survey (ERS) is the most suitable method for groundwater exploration among all other geophysical methods (Khalid et al., 2018; Farid et al., 2014). It is highly successful especially in the plain areas of interfluvial systems, where the difference between subsoil strata and saturated sediments exists (Khalid et al., 2019; McArthur et al., 2011; Telford et al., 1990). The electrical resistivity survey is used to measure the current and potential differences of diverse subsurface material at the surface (Okiongbo & Akpofure, 2016; Muchingami et al., 2012; Bowling et al., 2005; Robinson & Coruh, 1988).

The soil carries interstitial fluids and the current is conducted electrolytically in it. The electrical resistivity is influenced by grain size, water saturation, porosity, and dissolved salts. Clay minerals are capable to store the electrical charge. The current conducted in the clay minerals is electronic and electrolytic. So, the soil resistivity depends directly upon the clay minerals and electrolyte of soil and inversely related to porosity

---

S. Muhammad (✉) · P. Khalid (✉) · M. I. Ehsan  
Institute of Geology, University of the Punjab,  
Lahore 54590, Pakistan  
e-mail: geoshahbazmj@gmail.com

P. Khalid  
e-mail: pervez.geo@pu.edu.pk

S. Muhammad  
Geological Survey of Pakistan, Quetta, Pakistan

and fluid saturation (Fajana, 2020; Parasnis, 1986). Generally, the resistivity increases with the grain size. Thus, the resistivity increases in the following order of soil material such as clay, silt, sand, gravel, and boulder (Ochuk, 2011; Alile et al., 2008; Saleem, 1999; Borner et al., 1996).

The hydrogeological reconnaissance survey has its own importance to understand the hydrogeological setup of the area coupled with interpretation of ERS data (Khan et al., 2014; Kevin & Victor, 2014; Saleem, 2000). A detailed reconnaissance survey including field check of water samples within the study area was also carried out during the ERS.

The study area lies in the southwestern part of Bari Doab (between  $30.20^{\circ}$  N to  $30.65^{\circ}$  N and  $72.35^{\circ}$  E to  $72.90^{\circ}$  E), in most densely populated province Punjab. It lies within command area of Lower Bari Doab Canal (LBDC) which is the main source of irrigation in the area. Almost the whole area is comprised of agricultural land with an increasing demand of tube-well installation. The area is bounded by two rivers, Ravi River at North and Sutlej River at South: the main source of groundwater recharge. However, canals and rainfall are the secondary source of groundwater recharge (Bender & Raza, 1995; Kazmi & Jan, 1997).

The dependency on groundwater is escalating rapidly to meet the challenges like urban development, and agricultural and industrialization growth in the study area. The study area is arid to semi-arid climate zone with average annual rainfall recorded to be about 300 mm (Quraishi & Ashraf, 2019). Due to the effects of climatic changes, and the rainfall and groundwater conditions, the area has adversely been affected during last three decades (Malik et al., 2019). Eventually, the deterioration of quality and quantity of groundwater is being observed in different areas of Bari Doab and the study area as well. Hence, the monitoring of present aquifer conditions with different aspects, i.e., water table monitoring, identification of fresh-saline groundwater zones, and potential fresh groundwater zones, is the need of time.

The present study is an attempt to reinvestigate the hydrogeological conditions prevailing in the study area. In this research work, fresh, marginally fit, and saline/brackish groundwater zone have been delineated. In the light of the results of this study, the remedial steps can be taken for affected areas to rescue and even improve the groundwater quality by applying long-sighted industrial, agricultural, and urbanization policies, so that it would be a great service for better

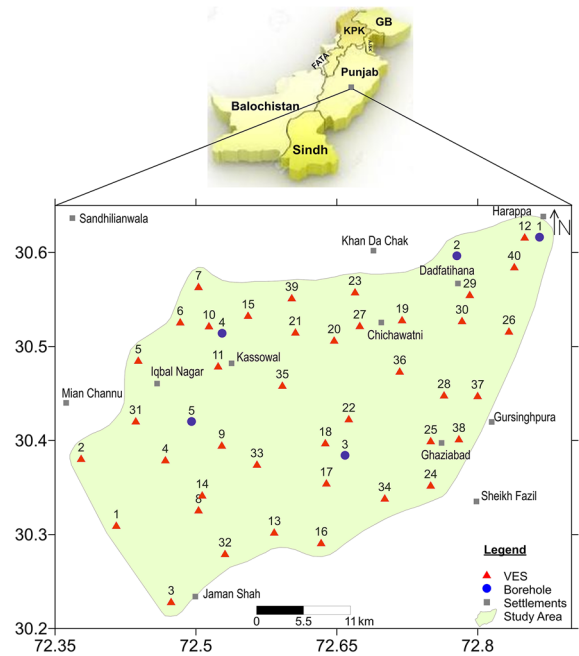


**Fig. 1** Base map of the study area showing VES and boreholes locations

future of the inhabitants. Moreover, the zones of quality groundwater identified during the study would be very beneficial to the inhabitants and agricultural point of view as well. A total of 40 vertical electrical resistivity profiles were conducted in the study area. The base map of the study area showing the locations of resistivity probes along with boreholes is shown in Fig. 1.

### Geology, geomorphology, and hydrology of the study area

The study area lies in central part of Bari Doab: a part of Indus Plain in Punjab Province of Pakistan. The Indus Plain is bounded by mountain ranges to the North and West, by the Arabian Sea to the South and the Thar Desert to the East. It is about 1200 km long and has a maximum width of about 400 km in the North. It is narrow in its central part and again becomes wider in its southern and lower part. Average slope of the plain is up to 1 m per 5 km and it is featureless except for the micro relief (Kazmi & Jan, 1997).

The Indus Plain is a complex geomorphologic unit and is composed of two broad geographical and geological

divisions, namely (a) the Piedmont zone, referred to as the Indus Piedmont, and (b) the Central Alluvial Plain, commonly referred to as the Indus Plain (Bender & Raza, 1995; Kazmi & Jan, 1997). The study area is the part of central alluvial plain within Bari Doab (Fig. 2). Bari Doab is deposited by existing and abandoned stream channels of Ravi and Sutlej Rivers. It is composed of unconsolidated alluvial deposits of Pleistocene to recent in age and is overlying the Precambrian basement rocks of Igneous/metamorphic complex. The alluvial cushion is very thick, and the exploratory drilling has revealed that Precambrian basement rocks are overlain by alluvium (Ahmad, 1974). The existing boreholes data in Bari Doab indicates that the alluvium cover is > 300 m thick and is composed mainly of silty clay, sand, sand-gravel, some kankar layers, and other fine silt. The lithological logs (Fig. 3) represent the major lithological distribution within the study area (Ali et al., 1982).

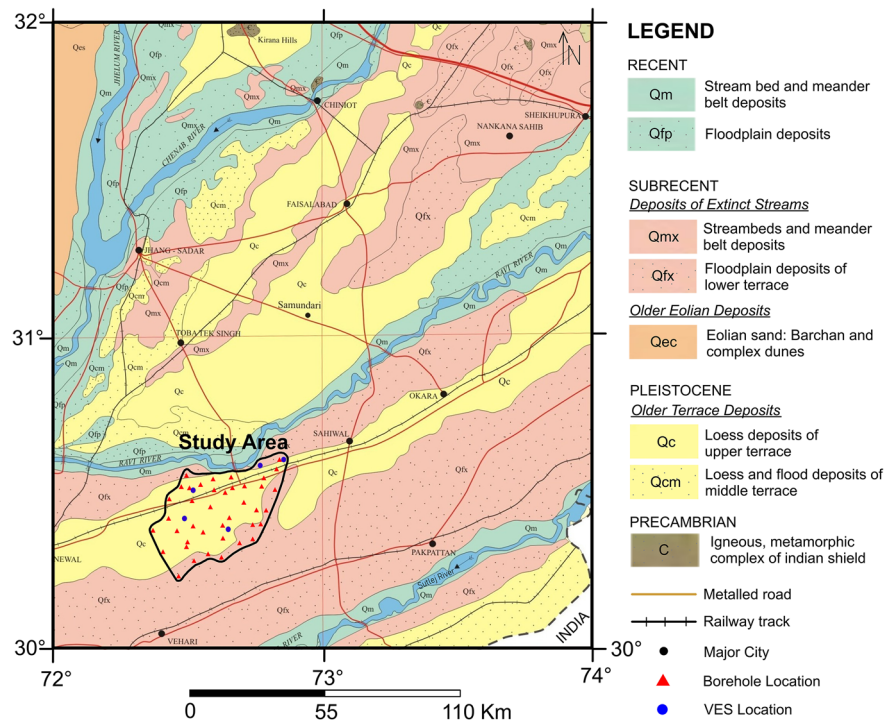
Conspicuous relief features in the Upper Indus Plain are a number of exposed monadnocks of the hard rocks near Sargodha, Chiniot, Sangla Hill, and Shahkot at neighboring Rachna and Jech Doabs (Ravi and Chenab

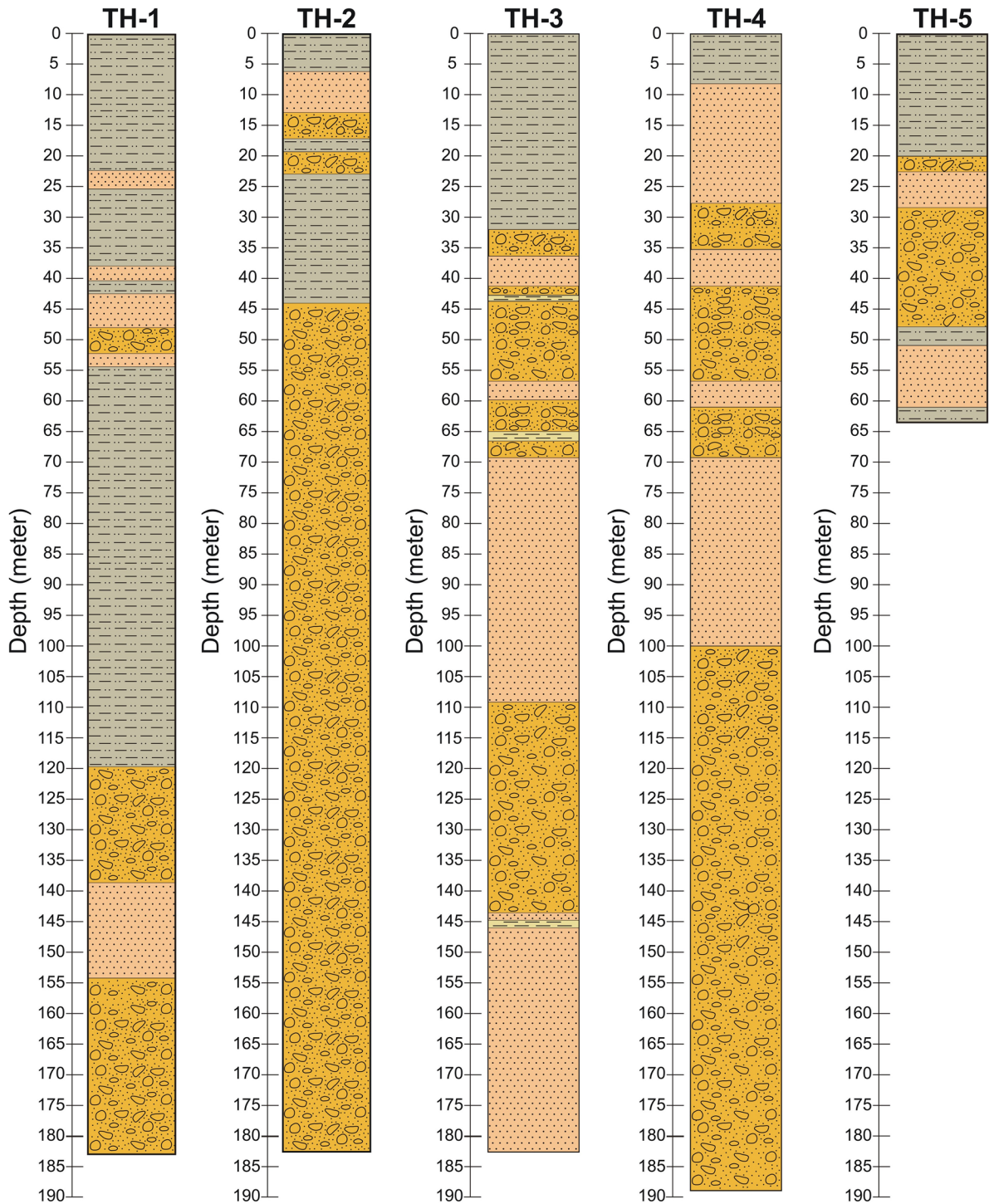
Rives, Jhelum and Chenab Rivers respectively) (Fig. 2). The Aravali Range of India is considered the continuity of these hills. In the North, these hills attain an altitude of about 250 m above sea level, their tops standing as much as 100 m above the plain (Kazmi & Jan, 1997).

The soil of Bari Doab is very productive under condition of fertilization and irrigation. It has medium to fine texture and low organic content. However, these soils are saline in some waterlogged areas (Ahmad, 1974; Malik et al., 2019).

The subsurface sandy deposits of alluvial complex form the zones of good-quality aquifers in which groundwater occurs under water table conditions. However, the presence of clayey layers has not been ascertained but presumably it is repeatedly reworked loess (Kazmi & Jan, 1997). The main cause of groundwater salinity is the subsurface clayey contents, which act as obstacles to the groundwater flow in the various parts of Bari Doab (Ahmad, 1974; Ahmad & Chaudhry, 1986; Ali et al., 1982; Malik et al., 2019). The surface geology in the study area (Fig. 2) is consisted of loess deposits (mostly silty clay) of upper terrace and flood plain deposits of

**Fig. 2** Regional and study area geology





**LEGENDS:-**



◀Fig. 3 Borehole lithological logs from the study area

lower terrace (Ahmad, 1974; Ahmad & Chaudhry, 1986; Ali et al., 1982; Bender & Raza, 1995; Kazmi & Jan, 1997; Malik et al., 2019; Quraishi & Ashraf, 2019).

**Methodology and dataset**

During the electrical resistivity survey, the direct current or low-frequency (< 1 Hz) current is infused within ground by using two current electrodes (denoted as A and B) firmly inserted in the ground. Between these two current electrodes, two potential electrodes (denoted as M and N) are inserted in the ground surface to measure the potential difference. During the whole survey, all the four electrodes are aligned along a straight line (Fig. 4) (Omosuyi et al., 2007; Robinson & Coruh, 1988; Telford et al., 1990).

By using the resistivity instrumentations, the current (*I*) flowing between current electrodes and the potential difference (*V*) between potential electrodes are measured (Kearey et al., 2002; Omosuyi et al., 2007). Hence, using Ohm’s law, the value of electrical resistivity ( $\rho$ ) is calculated as:

$$\rho = (K)(V/I) \tag{1}$$

$$K = \pi [(AB/2)^2 - (MN/2)^2] / MN \tag{2}$$

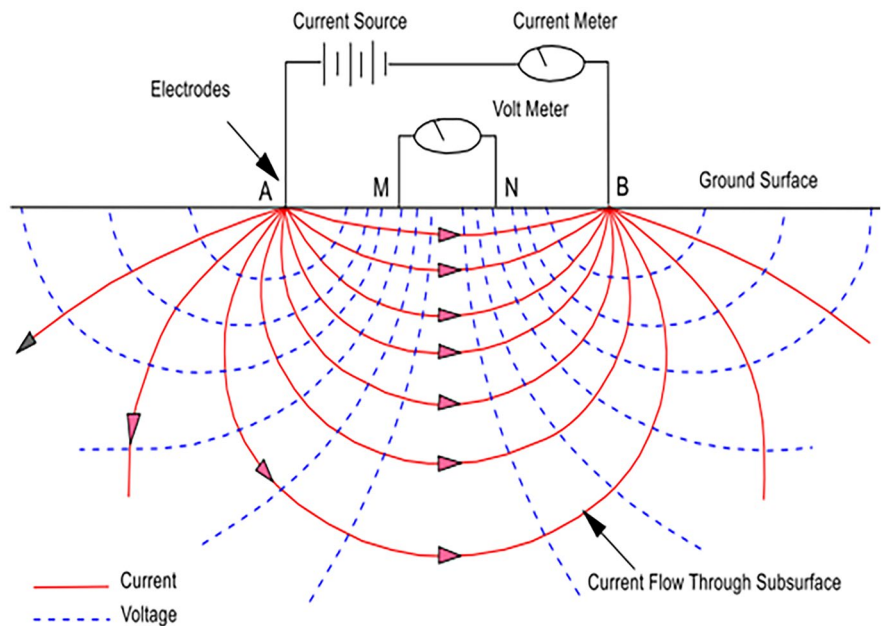
whereas *I* is the current (milliamperes), *V* is the potential difference (millivolts), and *K* is the geometric factor (depends upon the geometry of four electrodes).

In the isotropic and homogeneous subsurface conditions, the above relation gives true resistivity of the subsurface strata. But in nature, the subsurface material is anisotropic and the condition is not homogeneous. So, it represents a weighted average resistivity of the strata through which the current passes. Hence, the resistivity calculated from Eq. (1) is known as apparent resistivity ( $\rho_a$ ) (Kazakis et al., 2016; Kearey et al., 2002; Reynolds, 2011). Thus,

$$\rho_a = (K) (V/I) \tag{3}$$

The electrical resistivity of subsurface strata is related to the physical and chemical characteristics of pore fluid, mineral composition of sediments, porosity, and permeability of the sediments (Khalid et al., 2019; Muhammad & Khalid 2017; Farid et al., 2014; Ezomo & Ifedili 2006). Most of the electrical resistivity data acquisition was conducted in the study area in 2018 and 2019 by PCRWR. Later on, besides this, about 20% of electrical

**Fig. 4** Schematic diagram of electrical resistivity survey (Source: Robinson & Coruh, 1988)



resistivity data were also acquired by the authors to cover the non-acquired zones during field work in March 2020. All the data was acquired by using Tarameter, which records the value of resistance ( $V/I$ ) in milliohm ( $m\Omega$ ) or ohm ( $\Omega$ ). Vertical electric sounding (VES) was employed to study the resistivity variation with depth. In this technique, we expand the current and potential electrode spacing on ground during the field survey. The center of electrode array remains fixed at the observation point and the spacing between the electrodes is maintained. So, the apparent resistivity values are acquired for different depths below the surface (Akhter et al., 2012; Burger et al., 1992; Dobrin & Savit, 1988; Zananiri et al., 2006).

Among different electrode configuration, Schlumberger electrode configuration is the best for groundwater investigations. In this arrangement, the distance between current electrodes is large comparatively the distance between potential electrodes. So, the lateral in-homogeneities are easily identified (Kumar, 2019; Levanon & Ginzburg, 1976). Comparatively, this configuration needs less electrode spacing to achieve required investigative depth (Kumar, 2019; LaBrecque & Casale, 2002; Levanon & Ginzburg, 1976).

During the ERS data acquisition, a maximum current of 500 mA (keeping at auto mode) was infused into the surface with minimum 10 cycles by using a pair of stainless-steel electrodes inserted in ground with a fix distance along a straight line. Another pair of stainless-steel electrodes acts as potential electrodes also fixed between the current electrodes to receive current coming after going through the subsurface layers. Vertical electric soundings are conducted at sparsely distributed 40 observation points within the study area with half of current electrode spacing ( $AB/2$ ) ranging from 2 to 300 m. Hence, the maximum depth of investigation for all probes was 300 m. Half of current ( $AB/2$ ) and potential ( $MN/2$ ) electrode spacing, resistance ( $R$ ), geometrical factor ( $K$ ), and resultant apparent resistivity ( $\rho_a$ ) acquired at a single VES are presented in Table 1 as an exemplar. All the 40 VES were acquired in the same approach. The location and coordinates of VES points in the field were taken by using Global Positioning System. The acquired apparent resistivity data were then processed by using the software IPI2WIN.

Keeping high signal-to-noise ratio, the apparent resistivity readings were repeated at many stages during the data acquisition. The field data was acquired away

**Table 1** A typical VES field data of Schlumberger configuration

AB/2 (m)	MN/2 (m)	Resistance $R = V/I$ ( $\Omega$ )	Geometrical factor ( $K$ )	Apparent resistivity ( $\rho_a$ ) ( $\Omega m$ )
2	0.5	5.31	12	63.72
4	0.5	1.1	49	53.90
8	0.5	0.298	200	59.60
10	0.5	0.19	313	59.47
15	0.5	0.072	705	50.76
20	0.5	0.052	1255	65.26
25	0.5	0.037	1962	72.59
25	5	0.34	188	63.92
30	5	0.257	275	70.68
40	5	0.153	495	75.74
50	5	0.092	777	71.48
50	10	0.18	377	67.86
60	10	0.12	550	66.00
70	10	0.073	751	54.82
80	10	0.06	989	59.34
90	10	0.035	1256	43.96
100	10	0.025	1554	38.85
100	20	0.055	754	41.47
120	20	0.033	1100	36.30
150	20	0.021	1735	36.44
180	20	0.012	2512	30.14
210	20	0.0086	3430	29.50
240	20	0.0057	4490	25.59
270	20	0.0038	5691	21.63
300	20	0.00312	7034	21.95

from transmission lines, poles, railway tracks, and other underground utilities to avoid noise and to enhance reliability of the data. The geophysical interpretation is dependent upon the acquired field data. Therefore, during each of the reading taken by the instrument, the apparent resistivity values versus depth were plotted simultaneously on a logarithmic graph paper in the field. This practice is highly mandatory to ensure the smoothening trend of graph and to instantly retake the abnormal/misfit values of apparent resistivity.

The interpretation of resistivity data involves the curve matching technique. In this method, the field curve is compared with a set of standard curves or with the curves plotted with the computer program. The program curves and standard curves correspond to the subsurface layers and their electrical resistivity,

which could be correlated with the hydrogeological characteristics of that area (Akhter et al., 2012; Burger et al., 1992; Dobrin & Savit, 1988; Kazakis et al., 2016; Kearey et al., 2002; Reynolds, 2011; Zananiri et al., 2006).

## Results and discussions

To evaluate true resistivity model of each VES data set, a partial curve matching technique using auxiliary point method is used. A set of Ebert auxiliary graphs is used for this purpose. Final analyses of the resistivity curves are made by using the software IPI2WIN. In this research work, we have computed the earth layers model from the field data by using automatic iterative method. The apparent resistivity value in ohm meter (at  $Y$ -axis) and half of the distance between current electrodes ( $AB/2$ ) in meters (at  $X$ -axis) are taken as input data for the software. After the processing of apparent resistivity data, the true resistivity curves are generated for each VES probe. Some randomly selected processed graphs of VES-2, VES-26, VES-32, and VES-35 are shown in Fig. 5.

In Fig. 5, the apparent resistivity values are represented by small black circles. Considering the black line that joins the circles represents the apparent resistivity graphs taken in the field. The red line covering the circles is the focal line showing the processed data and represents the best fitted with the circles with a minimum root mean square shown on each processed graph. Moreover, the blue line with sharp edges is the resultant component of the graph. The horizontal portions of this line represent the thickness of a particular subsurface lithological layer. Hence, for each probe, the subsurface layers with their true resistivities and depths are evaluated. Each modeled layer is limited to a minimum number of lithological layers. A total of 4 to 6 geo-electric layers are interpreted in the study area. Each layer has a particular resistivity and thickness. The thickness of bottom layer cannot be identified because of limitation of maximum depth of investigation. A subsurface correlation of interpreted lithology with their true resistivities is developed by analyzing the processed curves of all the VES probes and borehole lithological logs collectively (Table 2). For interpretation, the true resistivities are calibrated by using lithological logs of nearby

boreholes (Fig. 6). The field observations, surface geology, field checks of groundwater samples, lithological logs of study area, information of water table depth, and literature review are integrally studied to compile the final interpretation.

The true resistivity values and thicknesses/depths of modeled layers of each probe obtained from processed graphs are tabularized, gridded, and plotted on base map to see the spatial distribution of resistivity in the study area. The 2D maps of true resistivity at depth of 2 m, 25 m, 50 m, 75 m, 100 m, 125 m, 150 m, 175 m, 200 m, 250 m, and 300 m are developed to delineate subsurface groundwater conditions (Fig. 7).

The resistivity values in the area are interpreted with a range of 0.12 to 770  $\Omega$ m. Water table in the area ranges from 7 to 26 m at different places. The resistivity value categorized for above and below the water table conditions.

Above the water table conditions, at depth of 2 m (Fig. 7a), very low resistivity values ( $<20 \Omega$ m) are interpreted as fine-grained dry sediments composed of silty clay with some organic content. As the resistivity increases ( $>20 \Omega$ m), the coarseness of the sediments also increases. So, the low resistivity values (20–40  $\Omega$ m) are interpreted as coarsening of dry sediments predominantly composed of silty clay with sand. Medium resistivity values ( $>40$ –100  $\Omega$ m) are interpreted as dry sediments mainly composed of medium to coarse sand with some gravel. High and very resistivity values ( $>100 \Omega$ m) are interpreted as sediments predominantly composed of dry sand.

At a depth of 25 m (Fig. 7b), the hydrogeological conditions are just below the water table. At this depth, the very low resistivity values ( $<20 \Omega$ m) are interpreted mainly as sand, sand with gravel, and some segments of clayey content. These sediments are interpreted as saturated with saline water. By analyzing very low resistivity zones in the map, the values decrease from 20  $\Omega$ m nearly up to zero. This is due to the effect of salinity in the groundwater. The low resistivity range (20–40  $\Omega$ m) is interpreted as saturated sediments predominantly of silty clay and sand. Groundwater is interpreted as marginally fair in this zone. Medium resistivity range ( $>40$ –100  $\Omega$ m) is interpreted as predominantly with medium to coarse sandy layers with some gravel and saturated with good quality water. High resistivity range ( $>100$ –230  $\Omega$ m) is interpreted as sandy layers with more gravel content and saturated with good-quality water also.

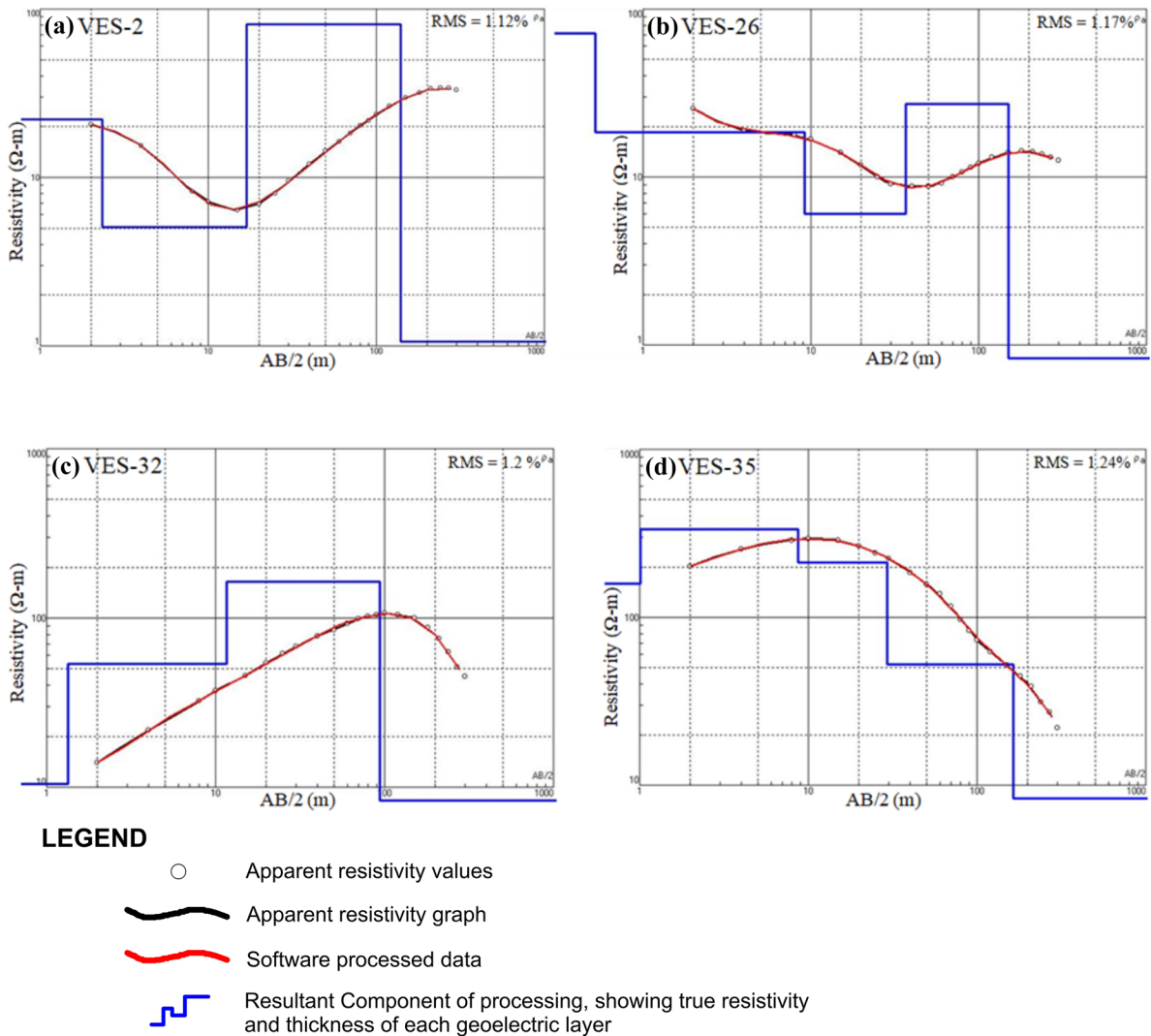


**Fig. 5** Processed graphs of VES-2, VES-26, VES-32, and VES-35 showing apparent modeled and true resistivity curves against depth of investigation

Sand with gravel and some stiff kankar inclusion are interpreted as to be associated with high resistivity value ( $> 230 \Omega\text{m}$ ).

At depth of 50 to 300 m (Fig. 7c–k), the zones of very low resistivity ( $< 20 \text{ m}$ ) are detected in the study area (shown with gray color) in which the resistivity value decreases nearly to zero. This decrement is interpreted as salinity in the groundwater within the strata mainly composed of thick sandy and gravel segments. The zones of low resistivity ( $20\text{--}40 \Omega\text{m}$ ) are considered groundwater source of marginally fair

quality (shown with greenish shade) and the strata interpreted mainly as thick sandy, gravel, and silty clay segments (Fig. 7c–k). The zones of medium resistivity ( $> 40\text{--}100 \Omega\text{m}$ ) are considered groundwater of good quality (shown with light bluish shade) and the strata interpreted mainly as thick sandy and some gravel segments (Fig. 7c–g). The zones of high resistivity ( $> 100\text{--}230 \Omega\text{m}$ ) are also detected and again interpreted as groundwater source of good quality (shown with dark bluish shade) and the strata interpreted mainly as thick sandy and more gravel segments



**Table 2** Cutoff values of true resistivities with interpreted lithology

Resistivity range ( $\Omega\text{m}$ )	Resistivity zone	Interpreted lithology
<20	Very low	Above water table condition: Predominantly fine material, i.e., silty clay. Below water table condition: Predominantly sand, sand with gravel. Saturated with saline water.
20–40	Low	Predominantly dry sediments, i.e., alternating layers of silty clay, sand and saturated with marginally fair quality water below water table.
>40–100	Medium	Predominantly interbedded sandy layers with some gravel and saturated with good-quality water below water table.
>100–230	High	Predominantly interbedded sandy and gravel layers and good-quality water below water table.
>230	Very high	Predominantly interbedded dry (above water table) and saturated (below water table) sand-gravel with stiff kankar and some cementation.

(Fig. 7c–g). The greenish and bluish shades go to diminish, and grayish color dominates in the maps while the depth increasing below 25 m up to 300 m.

Stacking of all the maps in a perspective view below the water table condition is a typical 3D demonstration to understand the depth-wise groundwater conditions

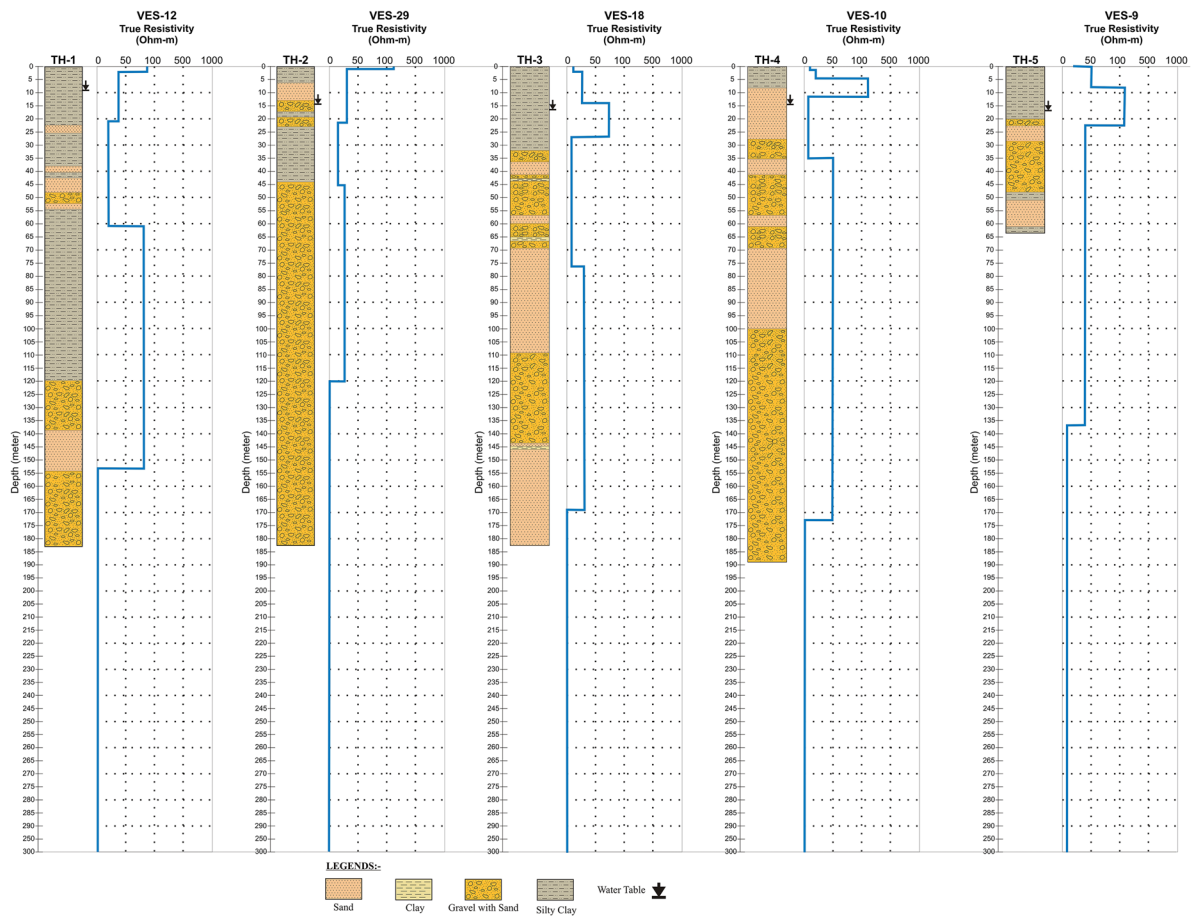


**Fig. 6** Calibration between borehole lithological logs and processed VES results

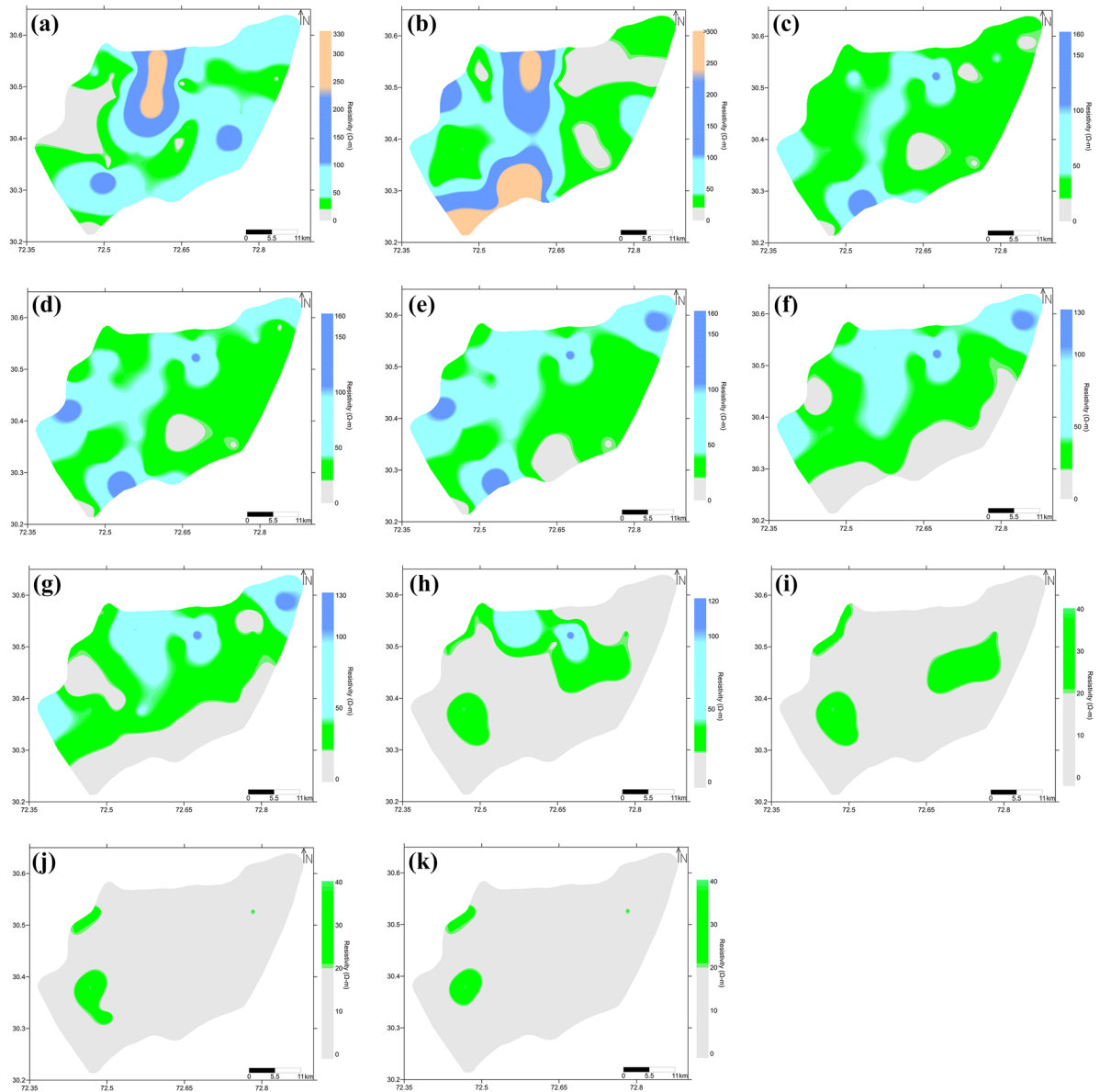


**Fig. 7** Modeled resistivity distribution maps at depth of **a** 2 m, **b** 25 m, **c** 50 m, **d** 75 m, **e** 100 m, **f** 125 m, **g** 150 m, **h** 175 m, **i** 200 m, **j** 250 m, and **k** 300 m

at subsurface (Fig. 8). The groundwater turns to saline as depth increase from 25 m.

For the understanding of hydrostratigraphy of the study area, the profile A-A' is selected on base map (Fig. 9). The cross-sections (Fig. 10) are generated along this profile using electrical resistivity processed data and data of borehole close to the profile. Along the profile, spatial distribution of electrical resistivity up to the maximum depth of investigation is

shown in Fig. 10a whereas the interpreted lithological cross-section is shown in Fig. 10b. The lithological cross-section (Fig. 10b) describes the 2D lithological variation along the profile. Under the water table conditions, the bluish (light blue and dark blue) shades (Fig. 10a) with medium and high resistivities, respectively ( $>40\text{--}230\ \Omega\text{m}$ ), are interpreted as good-quality water zones within sandy and gravel layers (Fig. 10b). The grayish color (Fig. 10b) with very low resistivities

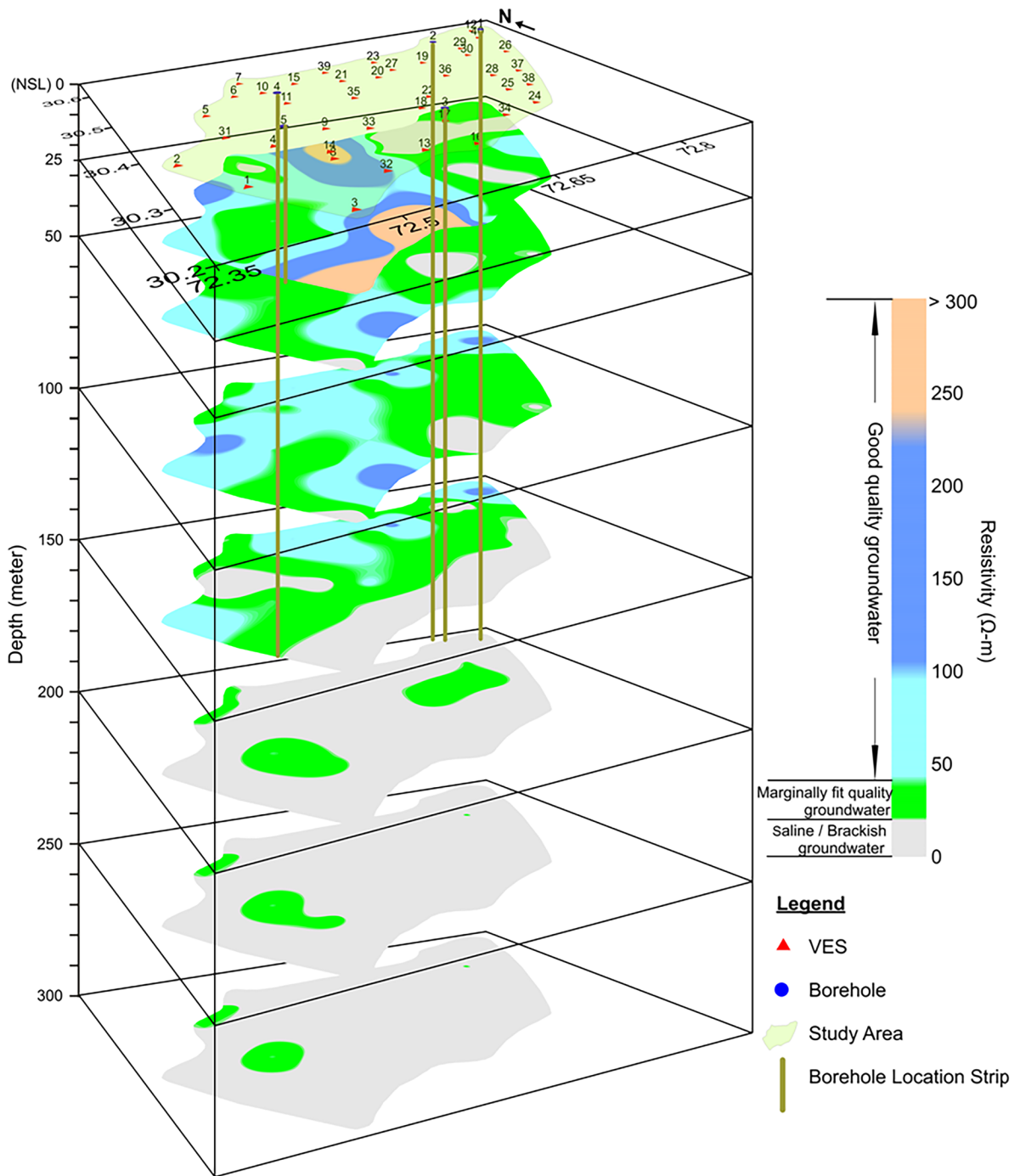


**Fig. 8** 3D Perspective view of stacked maps

(<20 Ωm) are interpreted as saline/brackish water zones mainly within the same sandy and gravel layers (Fig. 10b). The greenish shade (Fig. 10a) with low resistivities (20–40 Ωm), mainly within silty clay and

sand (Fig. 10b), is interpreted as marginally fair quality groundwater.

By analyzing the Figs. 7, 8, with Fig. 10 altogether, it is noticed that groundwater conditions go to saline

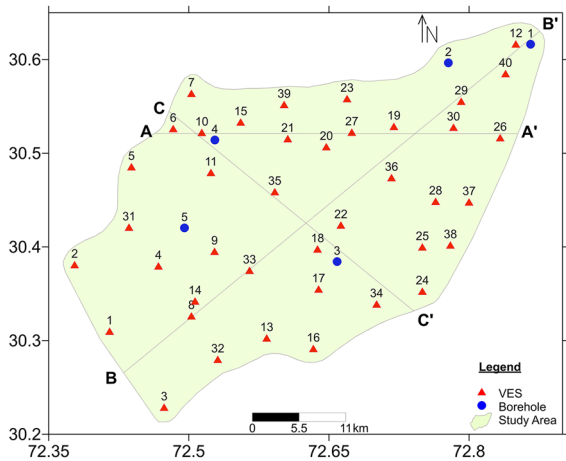


**Fig. 9** Base map representing the profiles A-A', B-B', and C-C'

from depth of about 150 m up to the maximum depth of investigation (300 m) except some small marginally fair quality groundwater pockets (Fig. 10).

Moreover, two more profiles B-B' and C-C' (Fig. 9) are selected across the study area. The depth section is generated to demonstrate the subsurface groundwater behavior under water table conditions. The 3D view of depth sections (Fig. 11) clearly deciphers that at depth of 25 m to about 150 m, groundwater potential

zones of good quality are present in the study area. However, salinity in groundwater perceived which goes to increase gently from the depth of 25 to 150 m and swiftly below the depth of 150 m. Furthermore, the groundwater goes to saline almost completely at the depth of 300 m. It is also inferred that the salinity persists below the maximum depth of investigation (300 m). The good-quality groundwater potential in the study area extends up to the depth of 150 m under water table conditions. The hydrogeological reconnaissance survey and calibration of lithological logs of the area also supports the interpreted results.

The main source of groundwater recharge in the study area is the River Ravi flowing parallel and adjacent to north of the study area. The other sources are LBDC crossing the study area and to some extent the precipitation. The north side of the study area holds good groundwater recharge due to the running water of River Ravi and recharge goes to decrease while moving away for the river towards south, although a huge zone of good/marginally fit groundwater extends up to 150-m depth (Fig. 7b–g). However, keeping the safer side to not to disturb the water balance, the groundwater may be exploited up to the depth of about 75 m within the interpreted good/marginally fit groundwater zones due to sufficient groundwater recharge at shallow levels (Fig. 7b–d). Up to this

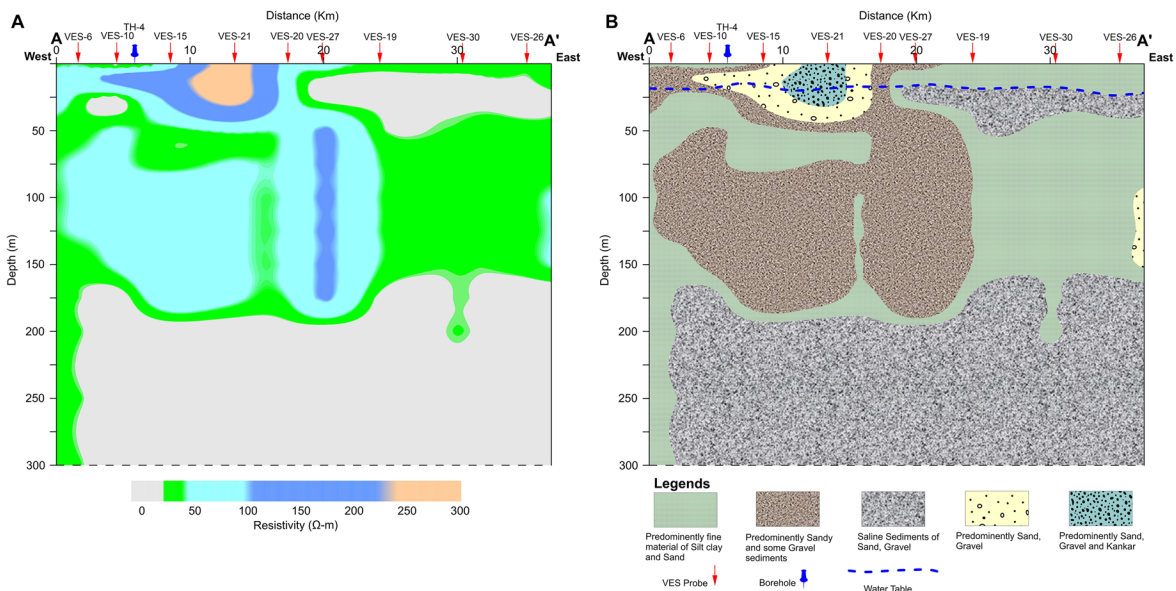
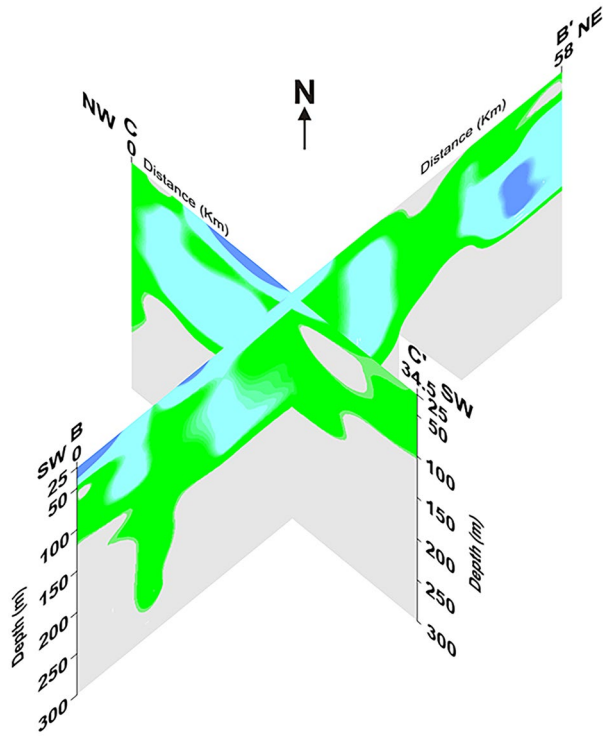


**Fig. 10** Along profile A-A' **a** electrical resistivity distribution and **b** lithological cross-section

**Fig. 11** 3D view of depth sections along profiles B-B' and C-C'



depth, groundwater should be exploited within interpreted zones of good and marginally fit groundwater and not within saline/brackish zones. Otherwise, it may cause to pollute the fresh groundwater zones

also. Below the depth of about 75 m, the groundwater may also be abstracted within the good/marginally fit zones but on account of a risk factor of water balance disturbance because of low groundwater recharge at

**Fig. 12** Groundwater resistivity distribution map of the study area

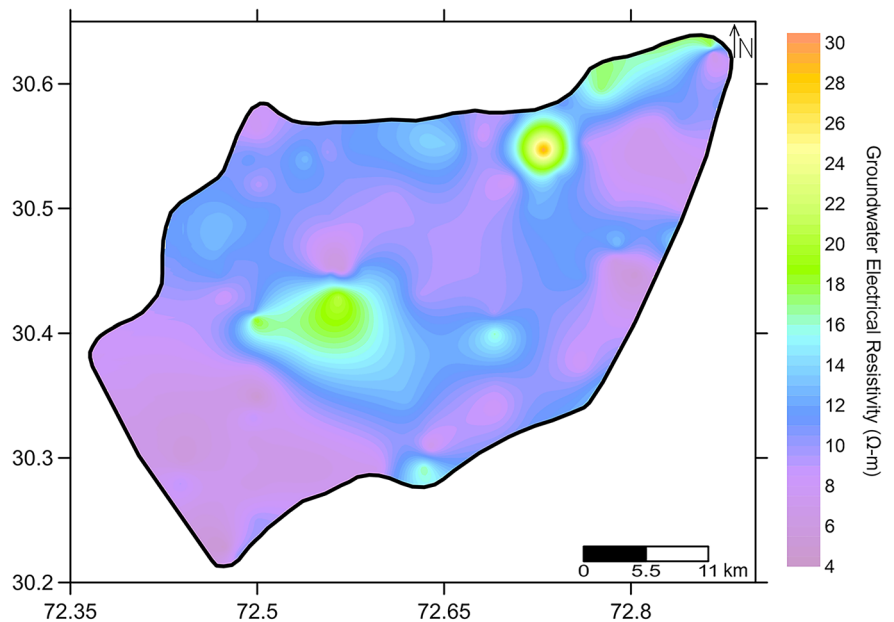
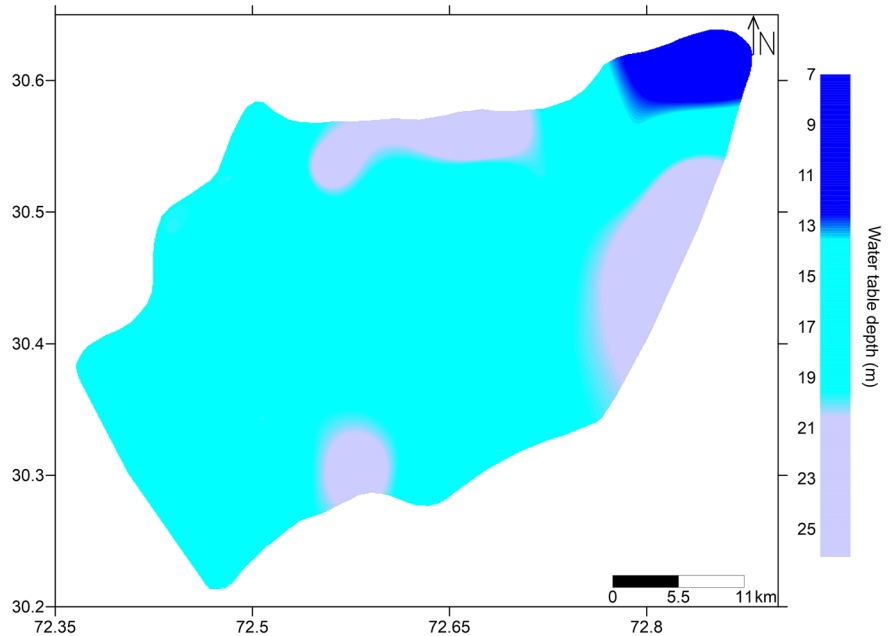


**Fig. 13** Water table depth map of the study area



deeper levels. Below the depth of 150 m (Fig. 7h–k), most of the study area turns to saline/brackish, so not fit for groundwater exploitation and may also cause the disturbance of water balance as well.

The salinity of groundwater can also be explained in terms of groundwater resistivity. For this purpose, about 97 groundwater samples were collected within the study area through different existing sources, i.e., hand pumps, open wells, motor pumps, and tube wells. These groundwater sources are installed at shallow depth up to 75 m averagely in the study area. So, the salinity behavior of groundwater up to this level is evaluated by obtaining the electrical conductivity values of these collected water samples and converting them into groundwater resistivity ( $R_w$ ). Finally, the groundwater resistivity map is generated and presented in Fig. 12 showing the groundwater resistivity distribution within the study area.

The water table depth map is (Fig. 13) prepared by using water table data taken at sparsely distributed 50 sites of hand pumps, tube wells, and motor pumps. Kriging method of interpolation was used to interpolate the values between these sparsely distributed sites. The water table in the study area varies from the depth of 7 to 26 m. The River Ravi is flowing at north side and almost parallel to the study area. At northeast side of the map (Fig. 13), the water table is at its shallowest position almost 7 to 13 m. At the rest of the map, water

table is between 13 and 20 m and covering almost the whole of the study area except some zones where the water table is at its deepest position, i.e., 20 to 26 m.

## Conclusions

Geophysical investigations with electrical resistivity survey allied with lithological logs of boreholes, tube well data, and review of previous literature are used altogether for spatial appraisal of groundwater aquifer conditions in the southwestern part of district Sahiwal, a part of central Bari Doab. Based upon the geophysical data interpretation, 4 to 6 numbers of subsurface geo-electric layers with variable thicknesses have been identified. The subsurface strata are composed of a variety of fine to coarse-grained sediments such as silty clay, sand, gravel, and kankar.

Below the water table conditions, the very low resistivity values are interpreted mainly as sand-gravel with saline water. Low resistivity values are interpreted mainly as silty clay, sand with marginally fair quality water. Medium resistivity values are correlated with coarse sediments of sand with some gravel and saturated with good-quality water. Sand with more gravel strata show the high resistivity range while inclusions of stiff kankar in these strata rise up its resistivity, thus, categorized as very high resistivity.

The fresh groundwater exists at the depth of 25 to about 150 m at different locations within the area with medium resistivity range. Below this depth, groundwater turns to saline almost completely except some small marginally fair quality water pockets of low resistivity range. The severe salinity does not end up to the maximum depth of investigation (300 m); it rather persists even below the depth of 300 m.

The saline water zone is not fit for use of inhabitants and agricultural purposes as well. Due to over-exploitation of fresh groundwater for agriculture and urbanization, the salinity may increase because of intermingling of saline groundwater into fresh groundwater as it would flow towards the fresh groundwater zones to balance the saturation. It is recommended to avoid overexploitation of fresh groundwater and enhancing the reliance on canal irrigation system by developing more sophisticated local canal system.

**Acknowledgements** The authors pay the deepest regards to Mr. Waseem Raza and Mr. Naveed Iqbal whose valuable knowledge, assistance, cooperation, and guidance enabled us to compile this manuscript. We also pay the profound gratitude to the anonymous reviewers for their technical suggestions to improve this manuscript. PCRWR and WAPDA are also highly acknowledged for providing dataset used in the research work. The present study is related to Ph.D. research work of author Shahbaz Muhammad.

**Data availability** The data used in this manuscript is available on request.

**Declarations**

**Ethics approval and consent to participate** This article does not contain any studies with animals and human subjects. The authors confirm that all the research meets ethical guidelines and adheres to the legal requirements of the study region. Moreover, this manuscript has not been published previously in any form (partially or in full) and is not under consideration for publication elsewhere.

**Consent for publication** The authors declare that this manuscript does not contain any individual person’s data and material in any form.

**Conflict of interest** The authors declare no competing interests.

**References**

Ahmad, N., & Chaudhry, G. R. (1986). *Irrigated agriculture of Pakistan*. Shahzad Nazir Publishers.

Ahmad, N. (1974). Waterlogging and salinity problems in Pakistan. Waterlogging and salinity cell – irrigation drainage and flood control research council, Lahore.

Akhter, G., Farid, A., & Ahmed, Z. (2012). Determining the depositional pattern by resistivity–seismic inversion for the aquifer system of Maira Area, Pakistan. *Environmental Monitoring and Assessment*, 184, 161–170. <https://doi.org/10.1007/s10661-011-1955-4>

Ali, S. A., Sheikh, M. K., Mehmood, S. D., Rehman, S. U., & Abrar, A. J. (1982). Hydrogeological data of Bari Doab Vol-I. Directorate General of Hydrology, WAPDA, Lahore.

Alile, O. M., Amadasun, C. V. O., & Ebuomwan, A. I. (2008). Application of vertical electrical sounding method to decipher the existing subsurface stratification and groundwater occurrence status in a location in Edo North of Nigeria. *International Journal of Physical Sciences*, 3(10), 245–249. <https://doi.org/10.5897/IJPS.9000083>

Bender, F. K., & Raza, H. A. (1995). *Geology of Pakistan*. Salzweg-Passau Publisher.

Borner, F. D., Schopper, J. R., & Weller, A. (1996). Evaluation of transport and storage properties in the soil and groundwater zone from induced polarization measurements. *Geophysical Prospecting*, 44, 583–601. <https://doi.org/10.1111/j.1365-2478.1996.tb00167.x>

Bowling, J. C., Rodriguez, A. B., Harry, D. L., & Zheng, C. (2005). Delineating alluvial aquifer heterogeneity using resistivity and GPR data. *Groundwater*, 43(6), 890–903. <https://doi.org/10.1111/j.1745-6584.2005.00103.x>

Burger, H. R., Sheehan, A. F., & Jones, C. H. (1992). *Introduction to applied geophysics – exploring the shallow subsurface*. W. W. North & Company Ltd.

Dobrin, M. B., & Savit, C. H. (1988). McGraw-Hill Book Company, Singapore.

Ezomo, F. O., & Ifedili, S. O. (2006). Schlumberger array of vertical electrical sounding (VES) as a useful tool for determining water bearing formation in Iruokpen, Edo state. *Nigeria. Africa Journal of Science*, 9(1), 2195–2203.

Fajana, A. O. (2020). Groundwater aquifer potential using electrical resistivity method and porosity calculation: A case study. *Nriag Journal of Astronomy and Geophysics*, 9(1), 168–175. <https://doi.org/10.1080/20909977.2020.1728955>

Farid, A., Khalid, P., Jadoon, K. Z., & Jouini, M. S. (2014). The depositional setting of the late quaternary sedimentary fill in southern Bannu basin, northwest Himalayan fold and thrust belt Pakistan. *Environmental Monitoring and Assessment*, 186(8), 6587–6604. <https://doi.org/10.1007/s10661-014-3876-5>

Kazakis, N., Pavlou, A., Vargemezis, G., Voudouris, K. S., Soulios, G., Plikas, F., & Tsokas, G. (2016). Seawater intrusion mapping using electrical resistivity tomography and hydrochemical data. An application in the coastal area of eastern Thermaikos Gulf, Greece. *Science of the Total Environment*, 543, 373–387. <https://doi.org/10.1016/j.scitotenv.2015.11.041>

Kazmi, A. H., & Jan, M. Q. (1997). *Geology and tectonics of Pakistan*. Graphic Publishers.

Kearey, P., Brooks, M., & Hill, I. (2002). An introduction to geophysical exploration. Blackwell Scientific Publications.

Kevin, M. H., & Victor, F. B. (2014). Hydrogeology-principles and practice, 2nd Edition. Blackwell Scientific Publications.

Khalid, P., Sanaullah, M., Sardar, M. J., & Iman, S. (2019). Estimating active storage of groundwater quality zones in

- alluvial deposits of Faisalabad area, Rechna Doab. *Pakistan. Arabian Journal of Geosciences*, 12, 206. <https://doi.org/10.1007/s12517-019-4372-6>
- Khalid, P., Ullah, S., & Farid, A. (2018). Application of electrical resistivity inversion to delineate salt and freshwater interfaces in quaternary sediments of northwest Himalaya. *Pakistan. Arabian Journal of Geosciences*, 11(6), 1–11.
- Khan, A. D., Ghoraba, S., Arnold, J. S., & Luzio, M. D. (2014). Hydrological modeling of upper Indus basin and assessment of Deltaic ecology. *International Journal of Modern Engineering Research*, 4(1), 73–85.
- Kumar, U. (2019). Introduction to applied geophysics. Random Publications.
- LaBrecque, D. J., & Casale, D. (2002). Experience with anisotropic inversion for electrical resistivity tomography. Proceedings of the 2002 Symposium on the Application of Geophysics to Engineering and Environmental Problems. p. 11ELE6 (9 pp).
- Levanon, A., & Ginzburg, A. (1976). Determination of salt–water interface by electric resistivity depth soundings. *Hydrological Sciences Bulletin*, 21(4), 561–568. <https://doi.org/10.1080/02626667609491674>
- Malik, M. A., Ashraf, M., Ali, B., & Aslam, A. M. (2019). Soil physical and hydraulic properties of the upper Indus basin of Pakistan. *Pakistan Council of Research in Water Resources (PCRWR), Islamabad*. <https://doi.org/10.13140/RG.2.2.21104.00008>
- McArthur, S. A. Q., Allen, D. M., & Luzitano, R. D. (2011). Resolving scales of aquifer heterogeneity using ground penetrating radar and borehole geophysical logging. *Environment and Earth Science*, 63(3), 581–593. <https://doi.org/10.1007/s12665-010-0726-9>
- Muchingami, I., Hlawtwayo, D. J., Nel, J. M., & Chum, C. (2012). Electrical resistivity survey for groundwater investigations and shallow subsurface evaluation of the basaltic-greenstone formation of the urban. *Physics and Chemistry of the Earth*, 50–52, 44–51. <https://doi.org/10.1016/j.pce.2012.08.014>
- Muhammad, S., & Khalid, P. (2017). Hydrogeophysical investigations for assessing the groundwater potential in part of the Peshawar basin, Pakistan. *Environment and Earth Science*, 76, 494. <https://doi.org/10.1007/s12665-017-6833-0>
- Ochuk, A. (2011). Undergroundwater exploration of Oleh, Nigeria using the electrical resistivity method. *Scientific Research and Essays*, 6(10), 4295–4300. <https://doi.org/10.5897/SRE11.963>
- Okiongbo, K. S., & Akpofure, E. (2016). Hydrogeophysical characterization of shallow unconsolidated alluvial aquifer in Yenagoa and Environs, Southern Nigeria. *Arabian Journal for Science and Engineering*, 41, 2261–2270.
- Omosuyi, G. O., Adeyemo, A., & Adegoke, A. O. (2007). Investigation of groundwater prospect using electromagnetic and geoelectric sounding at Afunbiowo. *The Pacific Journal of Science and Technology*, 8, 172–182.
- Parasnis, D. S. (1986). *Principles of applied geophysics*. Chapman and Hall Publishers.
- Quraishi, R. H., & Ashraf, M. (2019). Water security issues of agriculture in Pakistan. Pakistan Academy of Sciences, Islamabad.
- Reynolds, J. M. (2011). *An Introduction to Applied and Environmental Geophysics* (2nd ed.). John Wiley & Sons.
- Robinson, E. S., & Coruh, C. (1988). *Basic exploration geophysics*. John Wiley & Sons.
- Saleem, H. S. (1999). Determination of fluid transmissivity and electric transverse resistance for shallow aquifers and deep reservoirs from surface well log electric measurements. *Hydrology and Earth System Sciences*, 3(3), 421–427. <https://doi.org/10.5194/hess-3-421-1999>
- Saleem, H. S. (2000). Modelling of lithology and hydraulic conductivity of shallow sediments from resistivity measurements using Schlumberger vertical electrical soundings. *Energy Sources*, 23(7), 599–618. <https://doi.org/10.1080/00908310119202>
- Telford, E., Geldart, W. M., & Sheriff, R. E. (1990). *Applied geophysics*. Cambridge University Press.
- Zananiri, I., Memou, T., & Lachanas, G. (2006). Vertical electrical sounding (VES) survey at the central part of Kos Island, Aegean, Greece. *Geosciences* 411–413.

**Publisher's Note** Springer Nature remains neutral with regard to jurisdictional claims in published maps and institutional affiliations.

Springer Nature or its licensor holds exclusive rights to this article under a publishing agreement with the author(s) or other rightsholder(s); author self-archiving of the accepted manuscript version of this article is solely governed by the terms of such publishing agreement and applicable law.